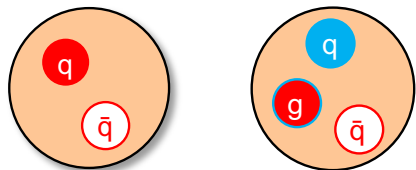


# Spin-Density Matrix Elements in the reaction $\gamma p \rightarrow \rho^- \Delta^{++}$ at GlueX

Niklas Herrmann for the GlueX collaboration

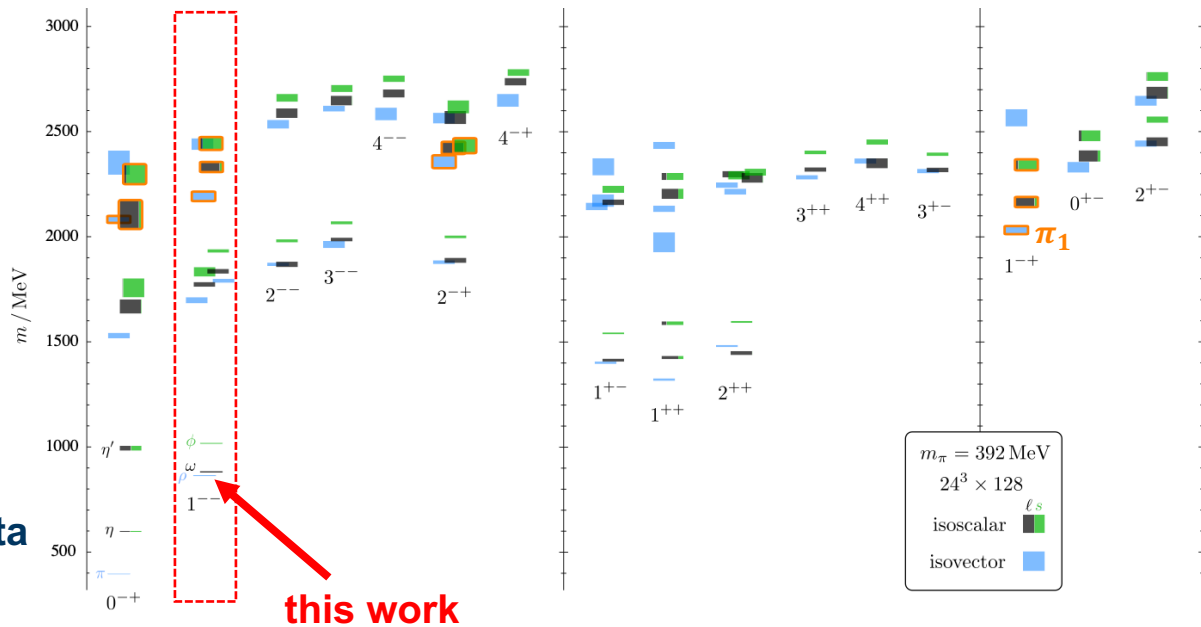
# Lattice QCD



- Goal of GlueX: map the full spectrum of light-quark mesons with an emphasis on **hybrid mesons** by using photoproduction
- Best evidence for gluonic excitations is for  $\pi_1(1600)$  in COMPASS pion-production data

Alexeev et al. (2022), *Phys. Rev. D* 105, 012005

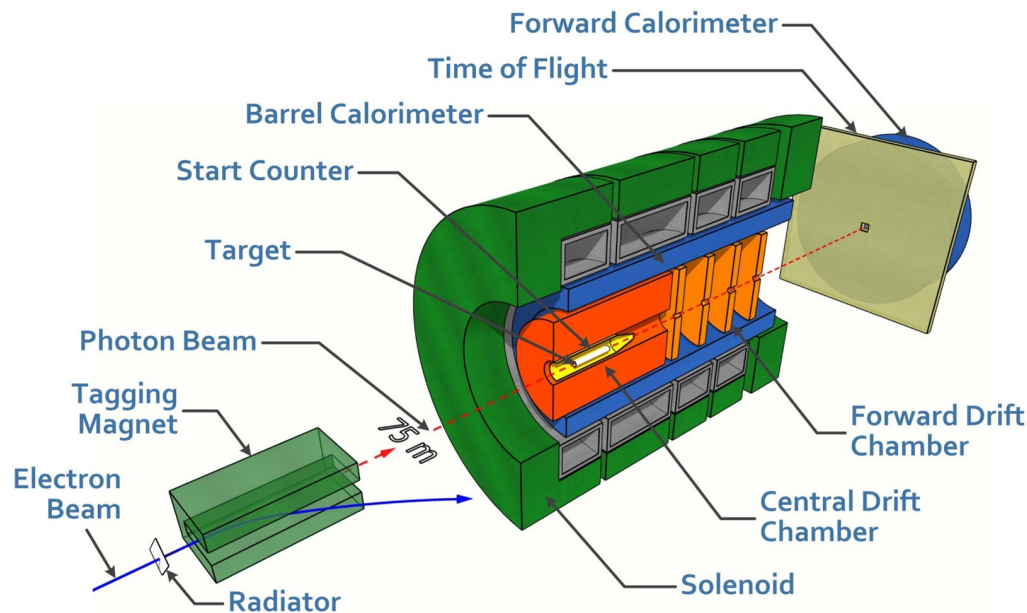
Dudek et al. (2013), *Phys. Rev. D*, 88, 094505



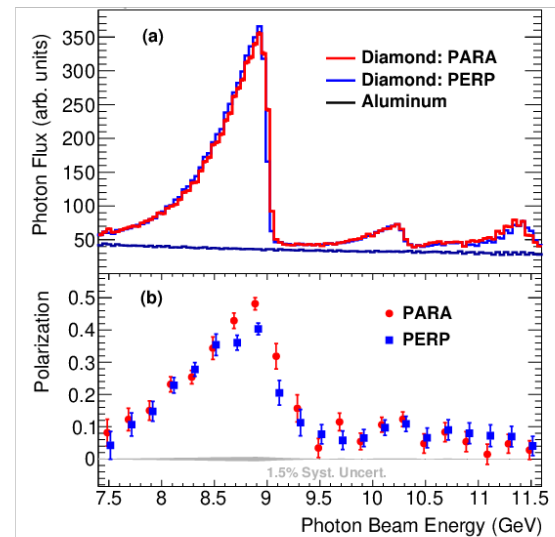
# GlueX experiment

F. Nerling (Thu, A2)  
H. Li (Fr, B3)  
I. Belov (Sat, A5)  
F. Afzal (Mo, plenary)  
M. Scott (Mo, B6)

MESON  
2026



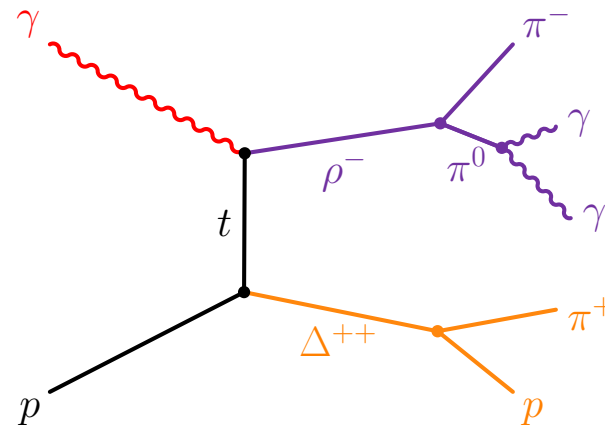
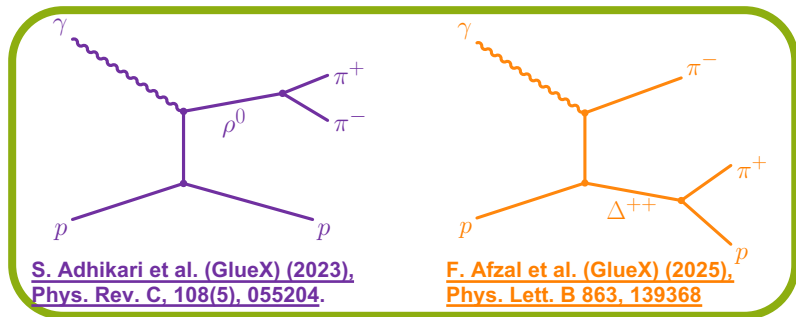
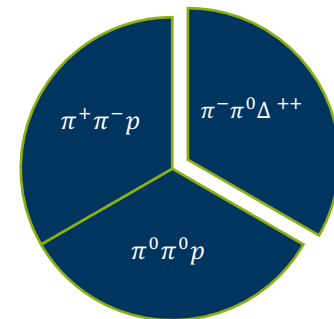
GlueX: NIMA 987 (2021) 164807



→ Experimental setup for light-quark meson spectroscopy providing nearly complete acceptance for charged and neutral particles in the final state

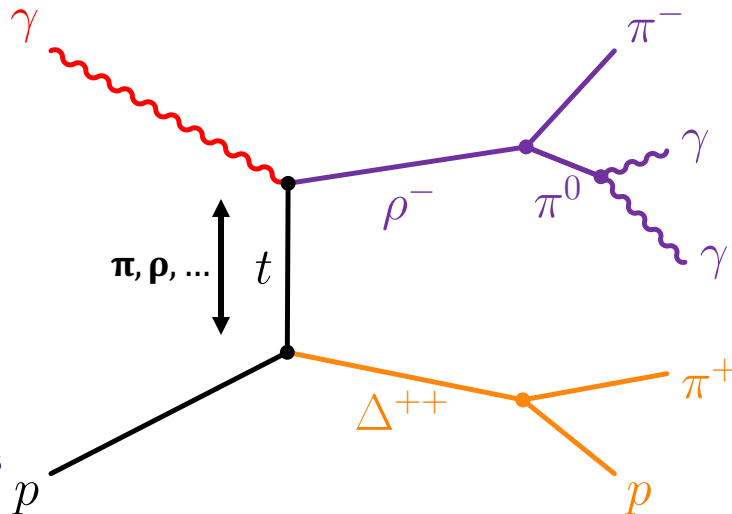
# Motivation for the reaction $\gamma p \rightarrow \rho^- \Delta^{++}$

- $\pi^+ \pi^- p$  and  $\pi^0 \pi^0 p$  states (neutral exchange) currently being analyzed by other collaborators
- $\pi^- \pi^0 \Delta^{++}$  (charge exchange, no isoscalar contribution) not studied yet
- Spin-Density Matrix describes the polarization of the produced Meson-Baryon system
- Goal: Determination of Spin-Density Matrix of  $\Delta^{++}$  and  $\rho^-$



# SDMEs

- SDMEs sensitive to the production mechanism
- Knowledge of the photon polarization enables the decomposition of the meson-baryon system spin-density matrix into its unpolarized and polarized components :  
 $\hat{\rho}^0$  (unpol),  $\hat{\rho}^1$  (linear)  $\hat{\rho}^2$  (linear)
- SLAC determined the unpolarized SDMEs in the 1970s



$$\vec{P}_\gamma = P_\gamma (-\cos(2\Phi), -\sin(2\Phi), 0)$$

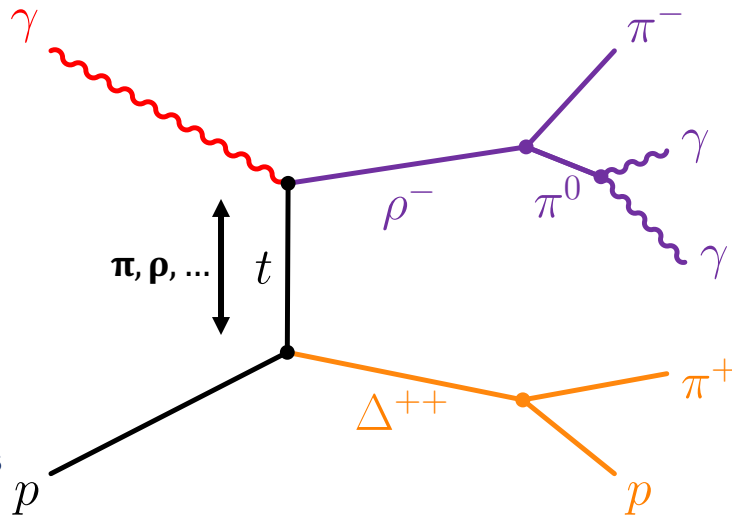
# SDMEs

$$\hat{\rho}_\gamma = \frac{1}{2} I + \vec{P}_\gamma \cdot \vec{\sigma}$$

- SDMEs sensitive to the production mechanism
- Knowledge of the photon polarization enables the decomposition of the meson-baryon system spin-density matrix into its unpolarized and polarized components :

$\hat{\rho}^0$  (unpol),  $\hat{\rho}^1$  (linear)  $\hat{\rho}^2$  (linear)

- SLAC determined the unpolarized SDMEs in the 1970s



$$\vec{P}_\gamma = P_\gamma (-\cos(2\Phi), -\sin(2\Phi), 0)$$

$$\hat{\rho}_{\rho-\Delta^{++}} = \hat{\rho}^0 + \sum_{\alpha=1}^3 P_\gamma^\alpha \hat{\rho}^\alpha$$

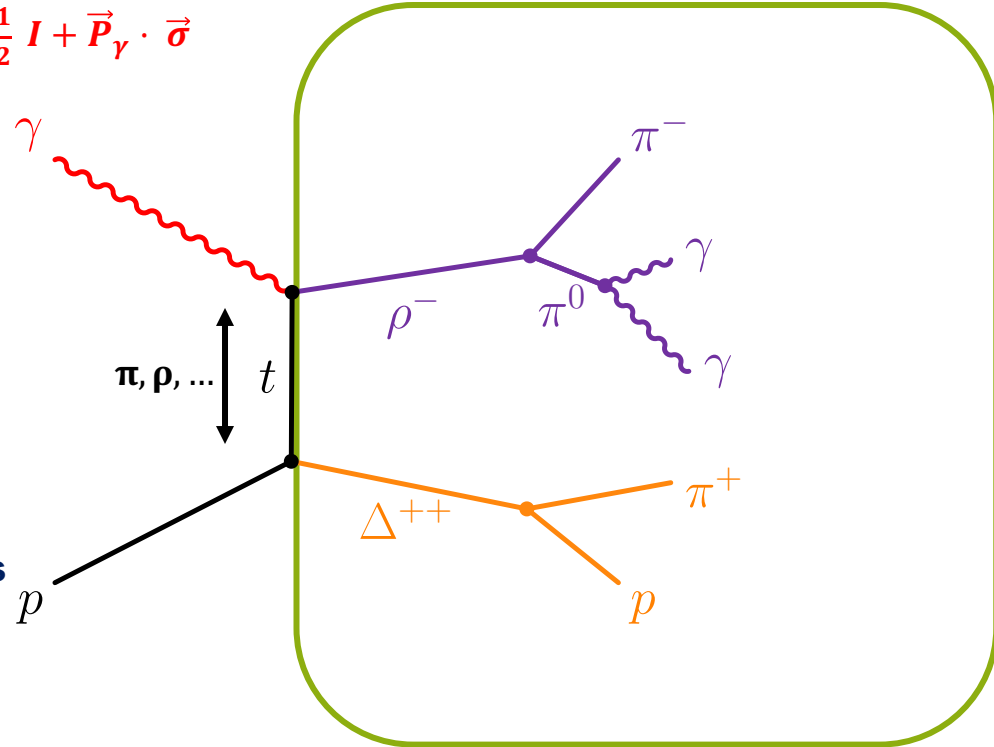
# SDMEs

$$\hat{\rho}_\gamma = \frac{1}{2} I + \vec{P}_\gamma \cdot \vec{\sigma}$$

- SDMEs sensitive to the production mechanism
- Knowledge of the photon polarization enables the decomposition of the meson-baryon system spin-density matrix into its unpolarized and polarized components :

$\hat{\rho}^0$  (unpol),  $\hat{\rho}^1$  (linear)  $\hat{\rho}^2$  (linear)

- SLAC determined the unpolarized SDMEs in the 1970s



$$\vec{P}_\gamma = P_\gamma (-\cos(2\Phi), -\sin(2\Phi), 0)$$

$$\hat{\rho}_{\rho^{-}\Delta^{++}} = \hat{\rho}^0 + \sum_{\alpha=1}^3 P_\gamma^\alpha \hat{\rho}^\alpha$$

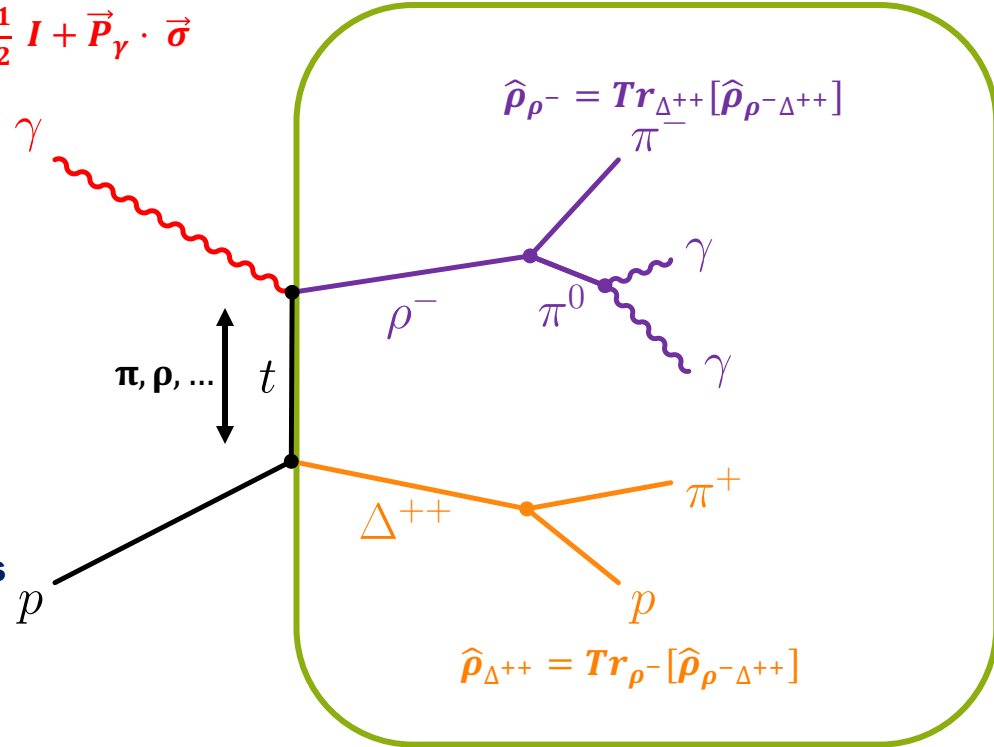
# SDMEs

- SDMEs sensitive to the production mechanism
- Knowledge of the photon polarization enables the decomposition of the meson-baryon system spin-density matrix into its unpolarized and polarized components :

$$\hat{\rho}^0 \text{ (unpol), } \hat{\rho}^1 \text{ (linear) } \hat{\rho}^2 \text{ (linear)}$$

- SLAC determined the unpolarized SDMEs in the 1970s

$$\hat{\rho}_\gamma = \frac{1}{2} I + \vec{P}_\gamma \cdot \vec{\sigma}$$



$$\vec{P}_\gamma = P_\gamma (-\cos(2\Phi), -\sin(2\Phi), 0)$$

$$\hat{\rho}_{\rho^-\Delta^{++}} = \hat{\rho}^0 + \sum_{\alpha=1}^3 P_\gamma^\alpha \hat{\rho}^\alpha$$

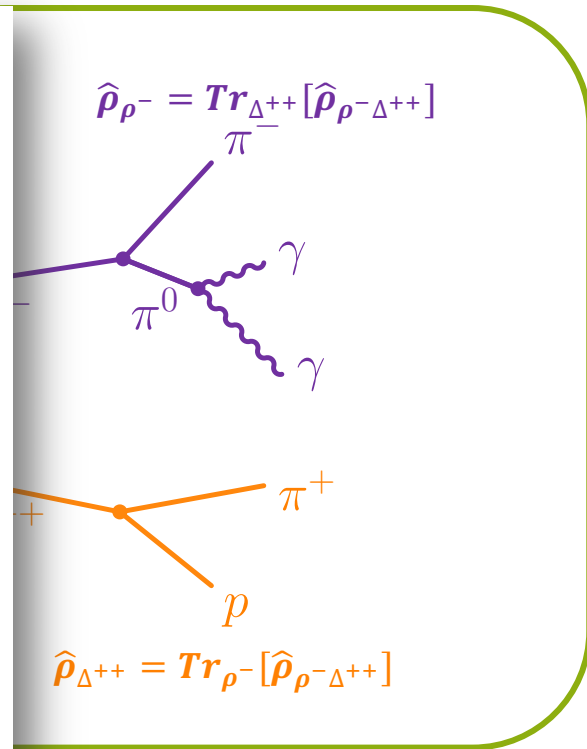
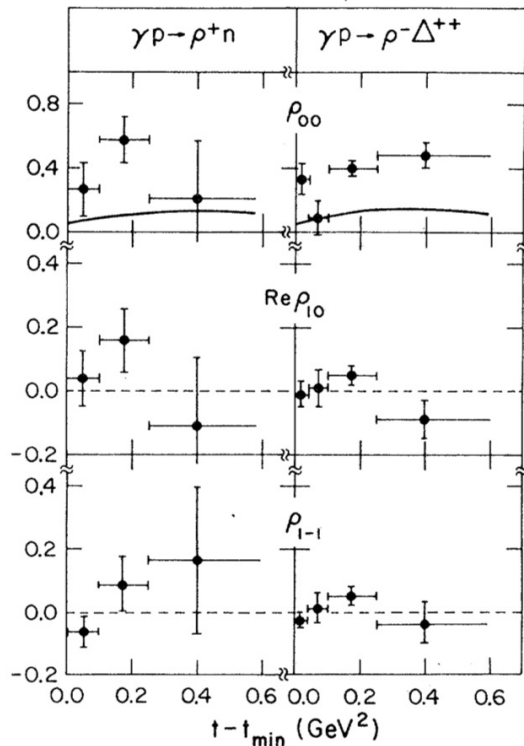
# SDMEs

- SDMEs sensitive to the production mechanism
- Knowledge of the production mechanism enables the decomposition of the meson-baryon system spin-density into unpolarized and polarized components

$$\hat{\rho}^0 \text{ (unpol)}, \hat{\rho}^1 \text{ (lin)}$$

- SLAC determined the SDMEs in the 1970s

J. Abramson et al. (1976), Phys. Rev. Lett., 36(24), 1432-1434.



# Event selection

# Mass windows

$$0.62 \text{ GeV} < M(\pi^- \pi^0) < 0.93 \text{ GeV}$$

$$1.10 \text{ GeV} < M(\pi^+ p) < 1.35 \text{ GeV}$$

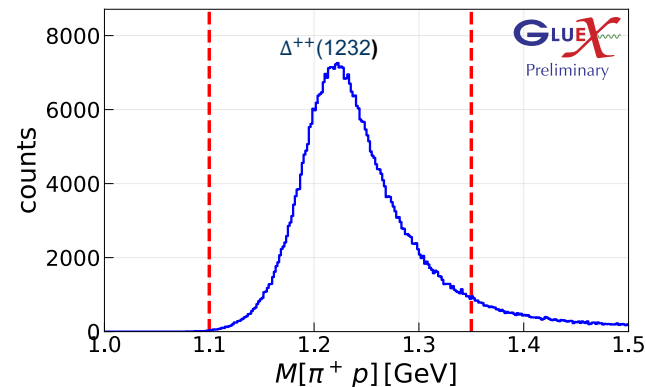
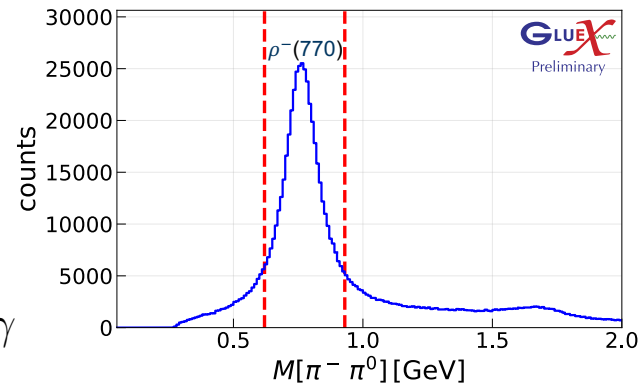
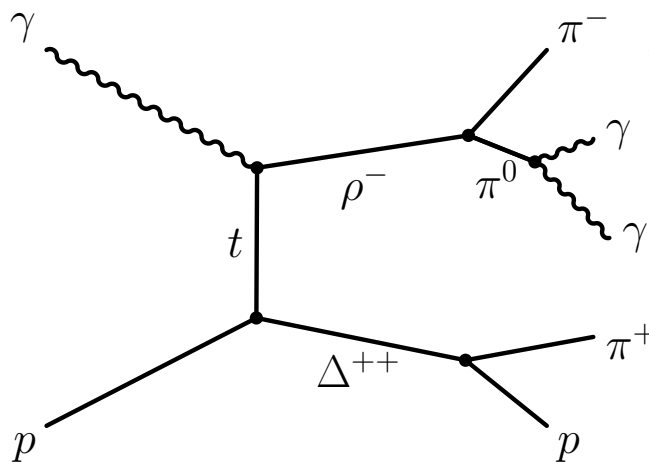
$$0.12 \text{ GeV} < M(\gamma\gamma) < 0.15 \text{ GeV}$$

$$0.9 \text{ GeV} < M(\pi^- \pi^0 \pi^+)$$

$$2.0 \text{ GeV} < M(\pi^0 p)$$

$$0.025 \text{ GeV}^2 < -t < 1.4 \text{ GeV}^2$$

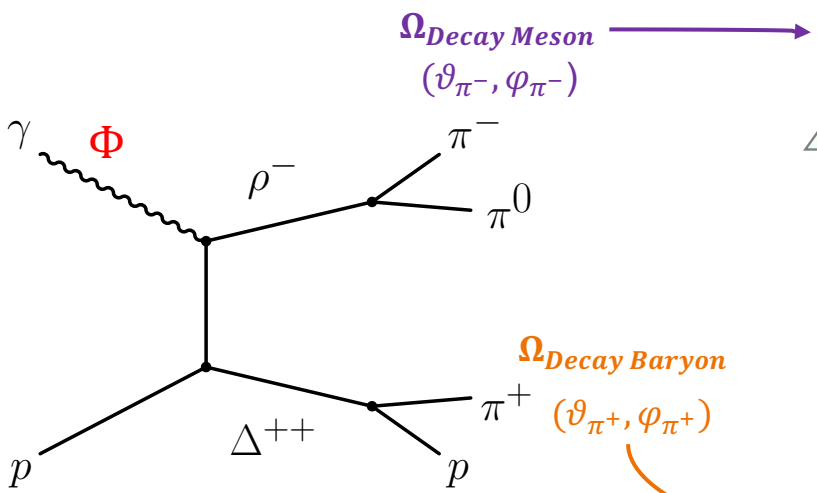
(16 bins in range)



- After the selection, a total of 1.8 million events remains for GlueX-I
- Background from different final states  $\sim 1.4\%$
- Combinatorial background  $< 1\%$  to  $14\%$  depending on  $-t$

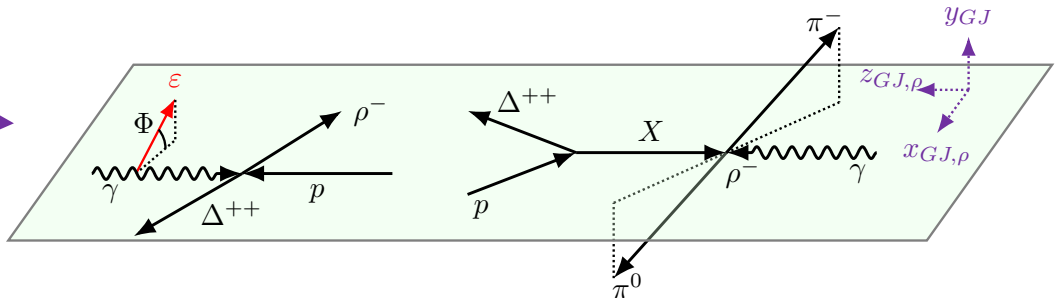
Fit to extract SDMEs

# Frames



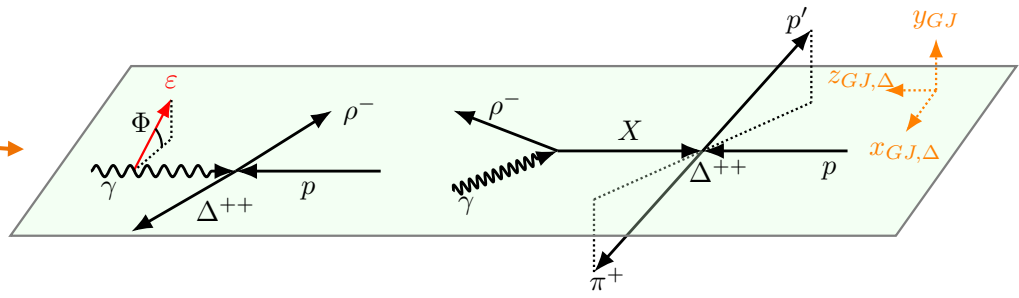
CM frame

$\rho^-$  Gottfried-Jackson (GJ) frame

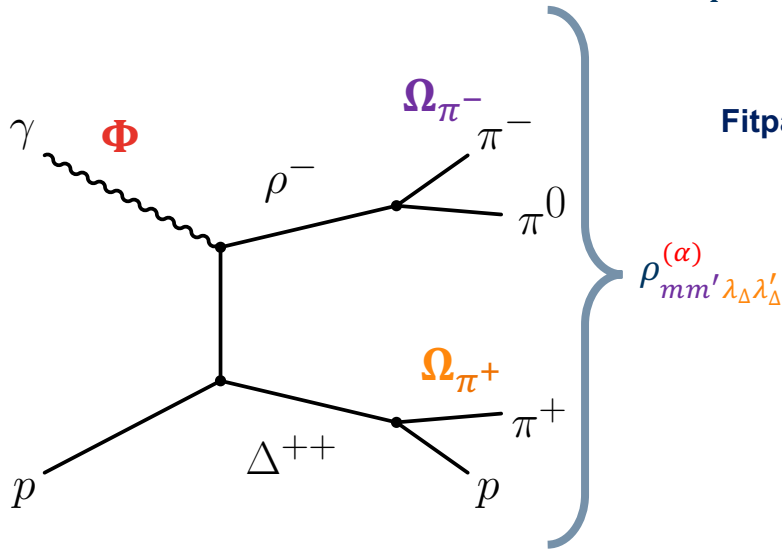


CM frame

$\Delta^{++}$  Gottfried-Jackson (GJ) frame



# Full fit model - Double SDMEs



$$I^\alpha = \frac{2\kappa}{\pi} \sum_{l,l'} \sum_{\lambda_\Delta, \lambda'_\Delta} \sum_{m,m'} |\tilde{F}(m_{\pi p}^2)|^2 c_{\lambda_\Delta \lambda'_\Delta}(\Omega_{\pi^+}) \rho_{mm', \lambda_\Delta \lambda'_\Delta}^{\alpha, l, l'}(s, t) c_{mm'}^{l, l'}(\Omega_{\pi^-}) |F(m_{\pi\pi}^2)|^2$$

Fitparameter  $r_{mm' \lambda_\Delta \lambda'_\Delta}^\alpha, \tilde{r}_{mm' \lambda_\Delta \lambda'_\Delta}^\alpha$  is a linear combination of one to four  $\rho_{mm' \lambda_\Delta \lambda'_\Delta}^\alpha$

Parity, hermicity, normalisation, linear combination

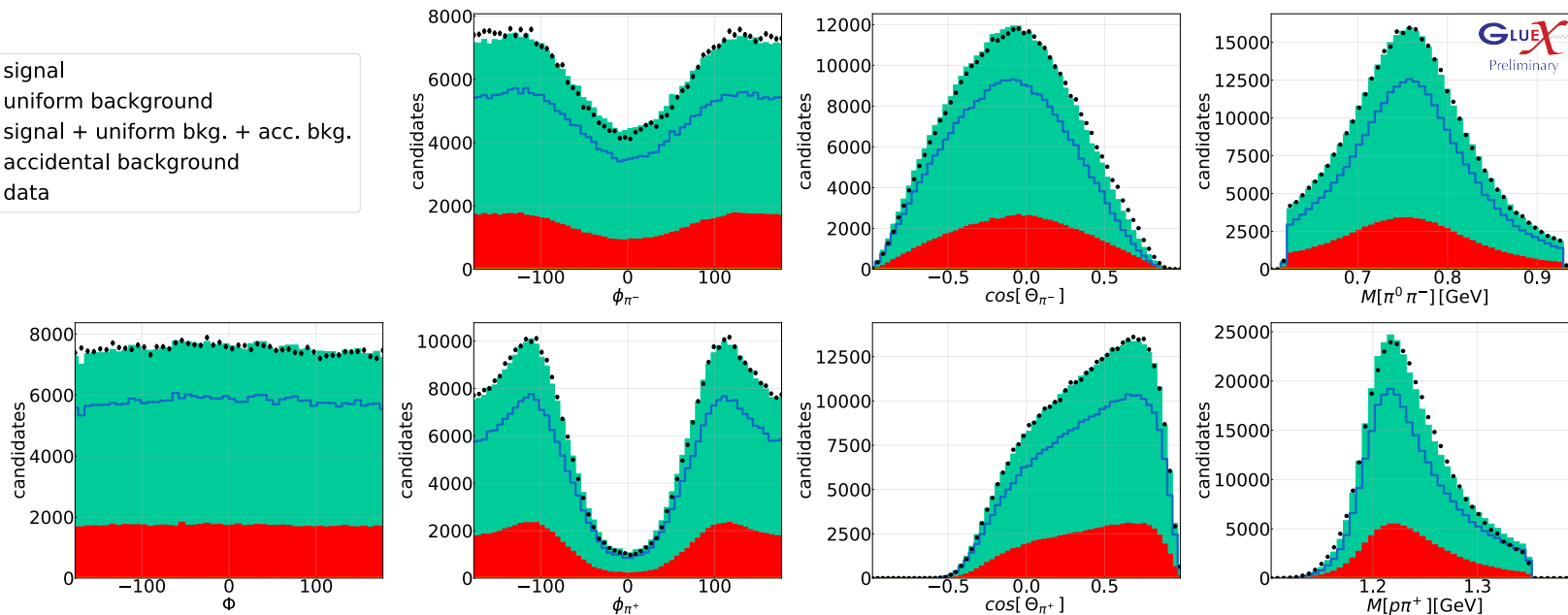
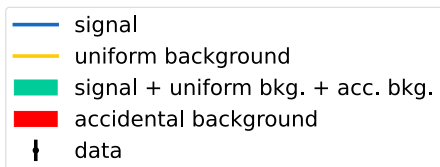
$\alpha = 0:$	19 fit parameters
$\alpha = 1:$	20 fit parameters
$\alpha = 2:$	16 fit parameters

Open question: do the upper and lower vertex factorize?

Factorization  $\Rightarrow \tilde{r}_{mm' \lambda_\Delta \lambda'_\Delta}^\alpha$  vanishes

# Fit Evaluation

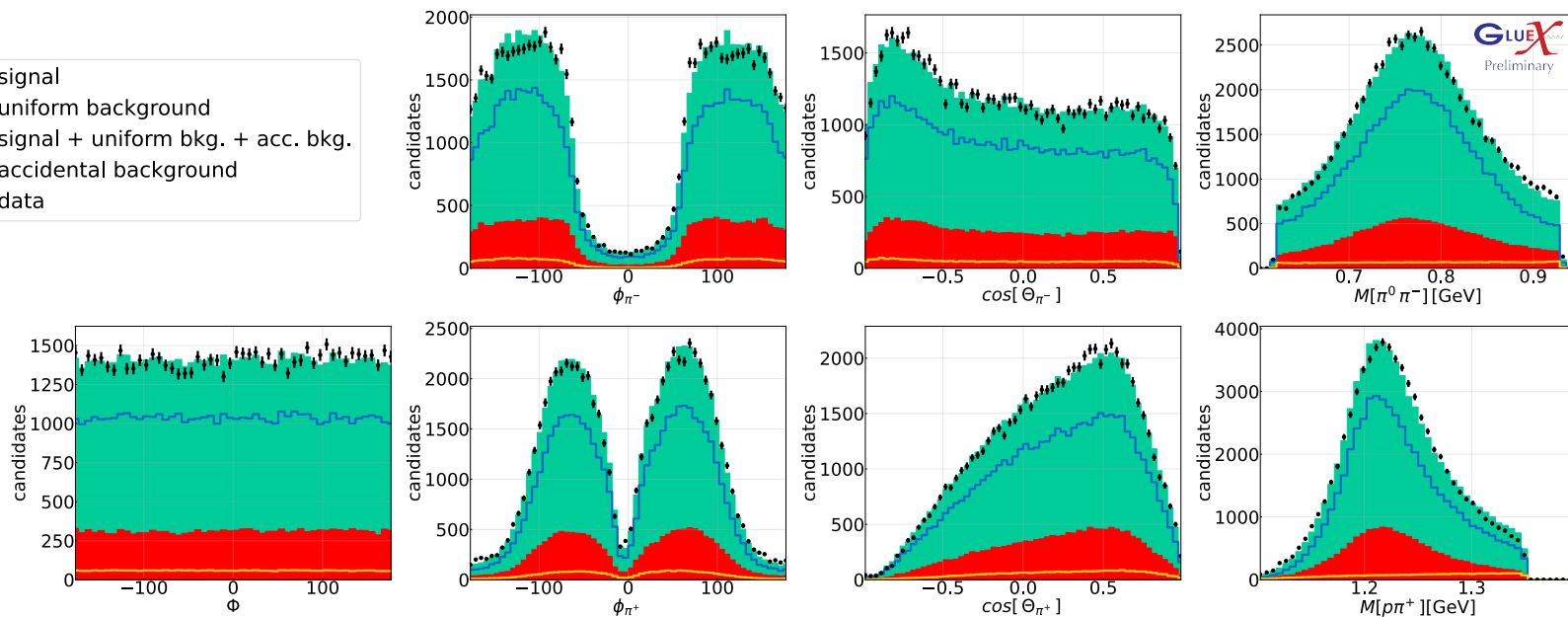
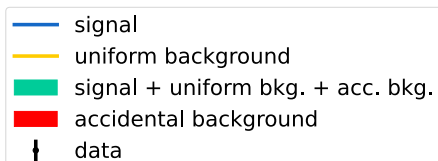
$0.025 \text{ GeV}^2 < |t| < 0.075 \text{ GeV}^2$



→ Overall very good agreement between data and fit

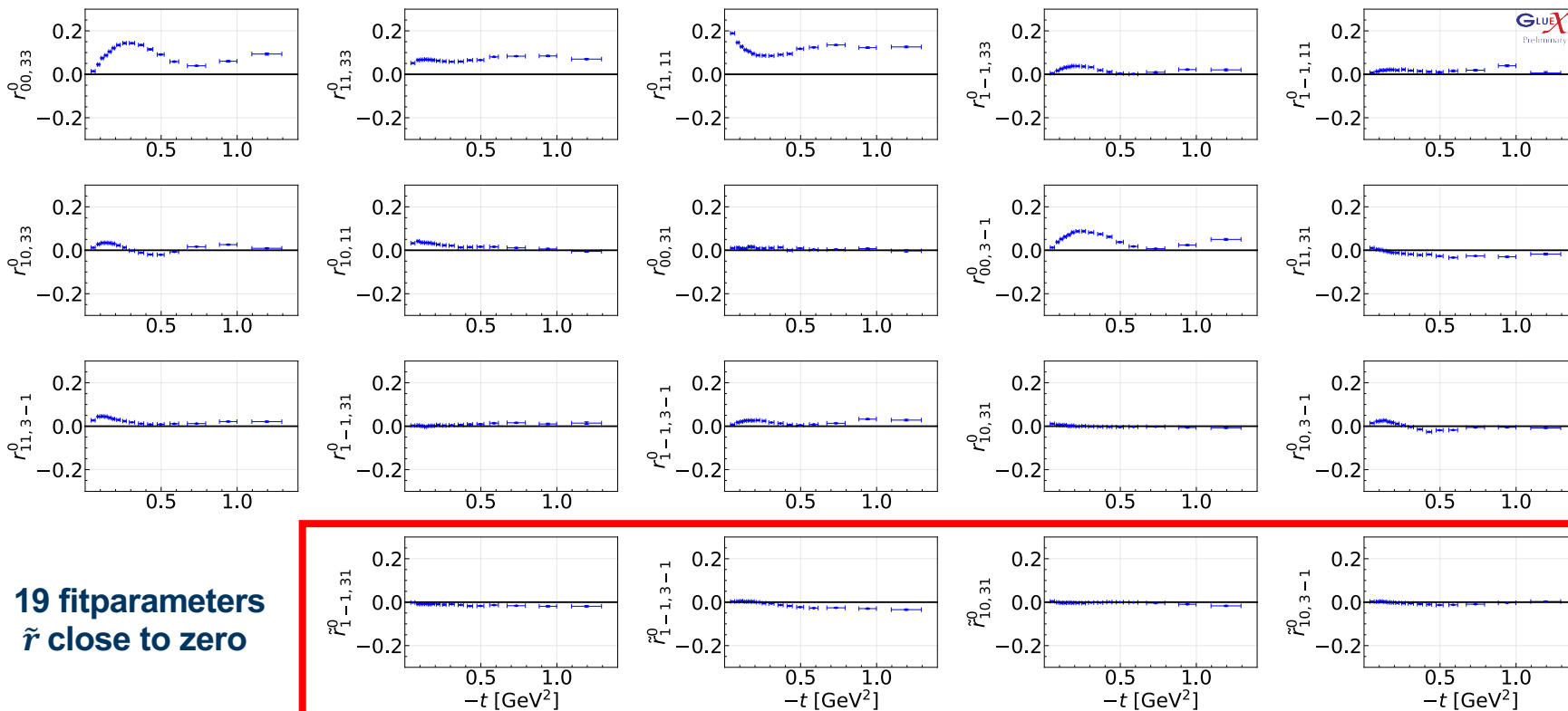
# Fit Evaluation

$0.460 \text{ GeV}^2 < |t| < 0.540 \text{ GeV}^2$



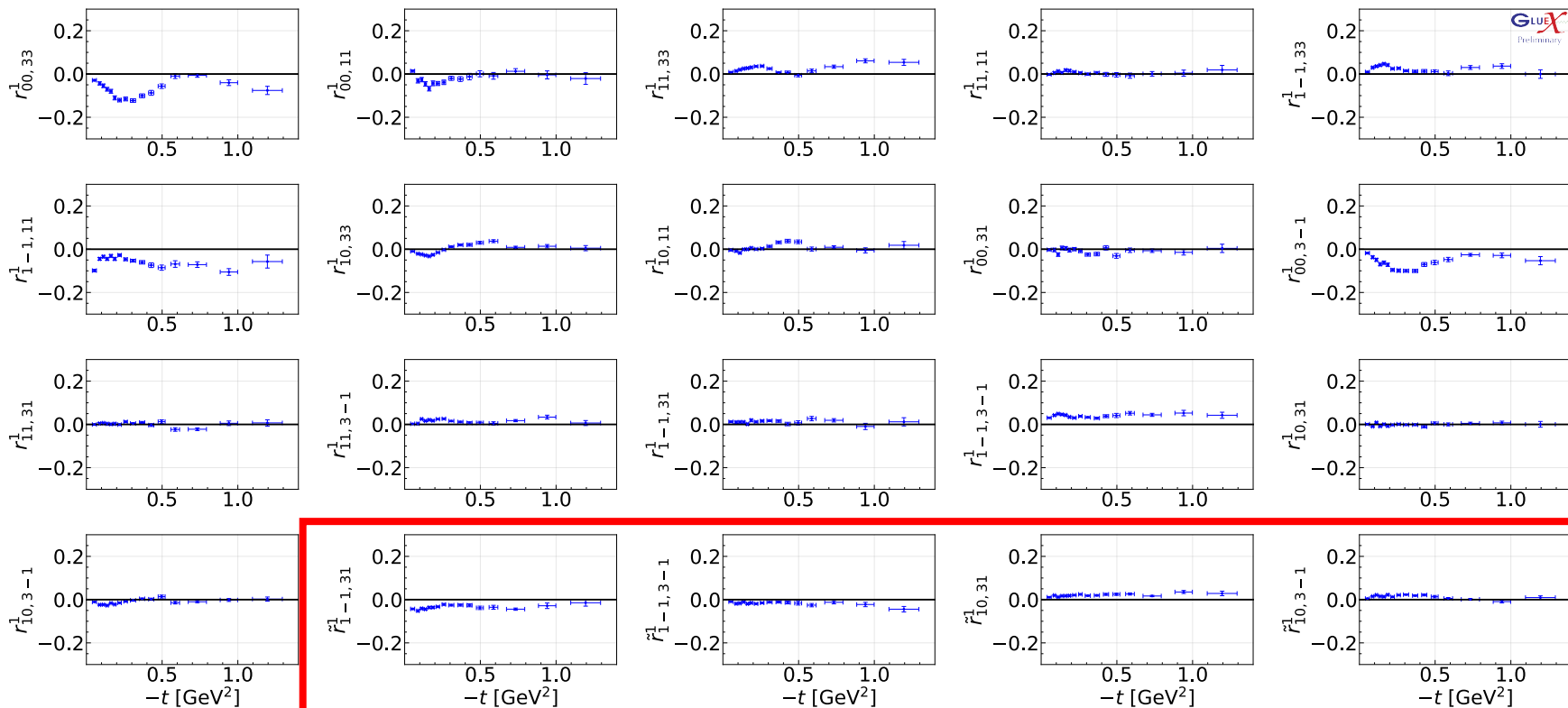
→ Overall very good agreement between data and fit (even for higher  $t$ -bins)

# Full model - unpolarized Double SDMEs

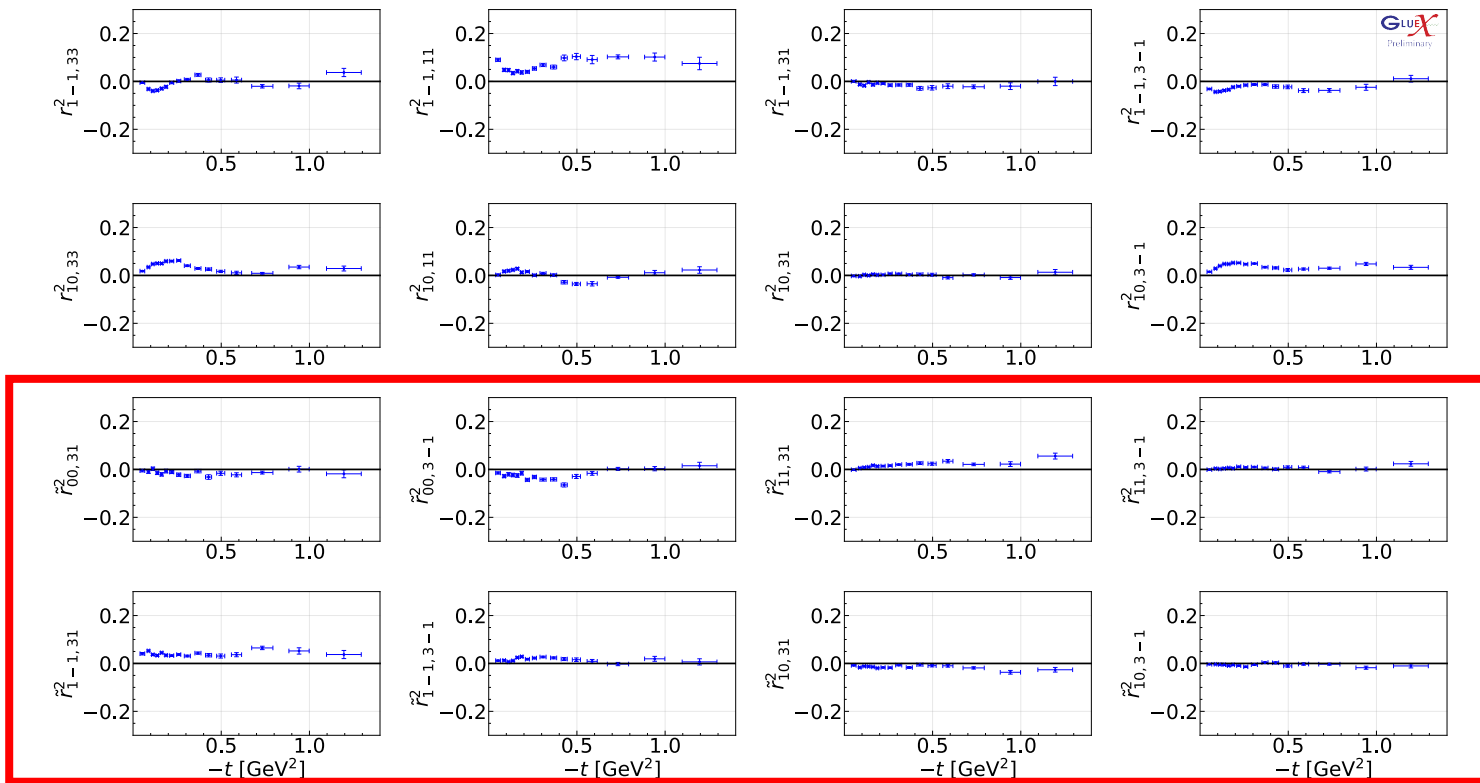


→ 19 fitparameters  
 →  $\tilde{r}$  close to zero

# Full model - polarized Double SDMEs ( $\alpha = 1$ )



# Full model - polarized Double SDMEs ( $\alpha = 2$ )



# Naturality

- Naturality is given by the quantum numbers  $J^P$  of the exchanged particle:

$$\eta = P(-1)^J$$

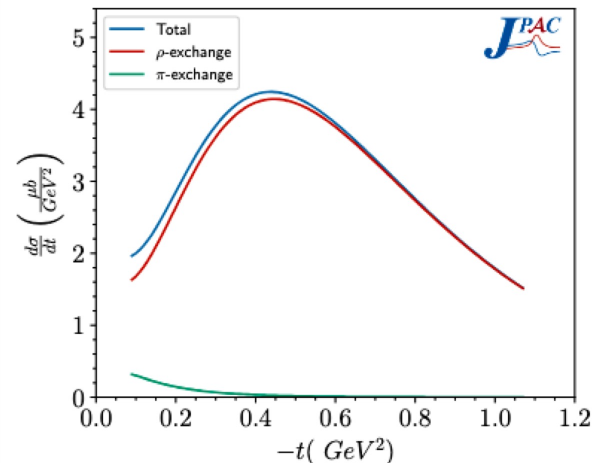
- Certain linear combinations of SDMEs allow separation of **natural** ( $\eta = 1$ ) and **unnatural** ( $\eta = -1$ ) exchange amplitudes

$$r_{1-1,33}^0 + r_{11,33}^1 = 2 \operatorname{Re}(N_{1,-3} N_{-1,-3}^* + N_{1,3} N_{-1,3}^*) \quad (\text{purely natural exchange amplitudes})$$

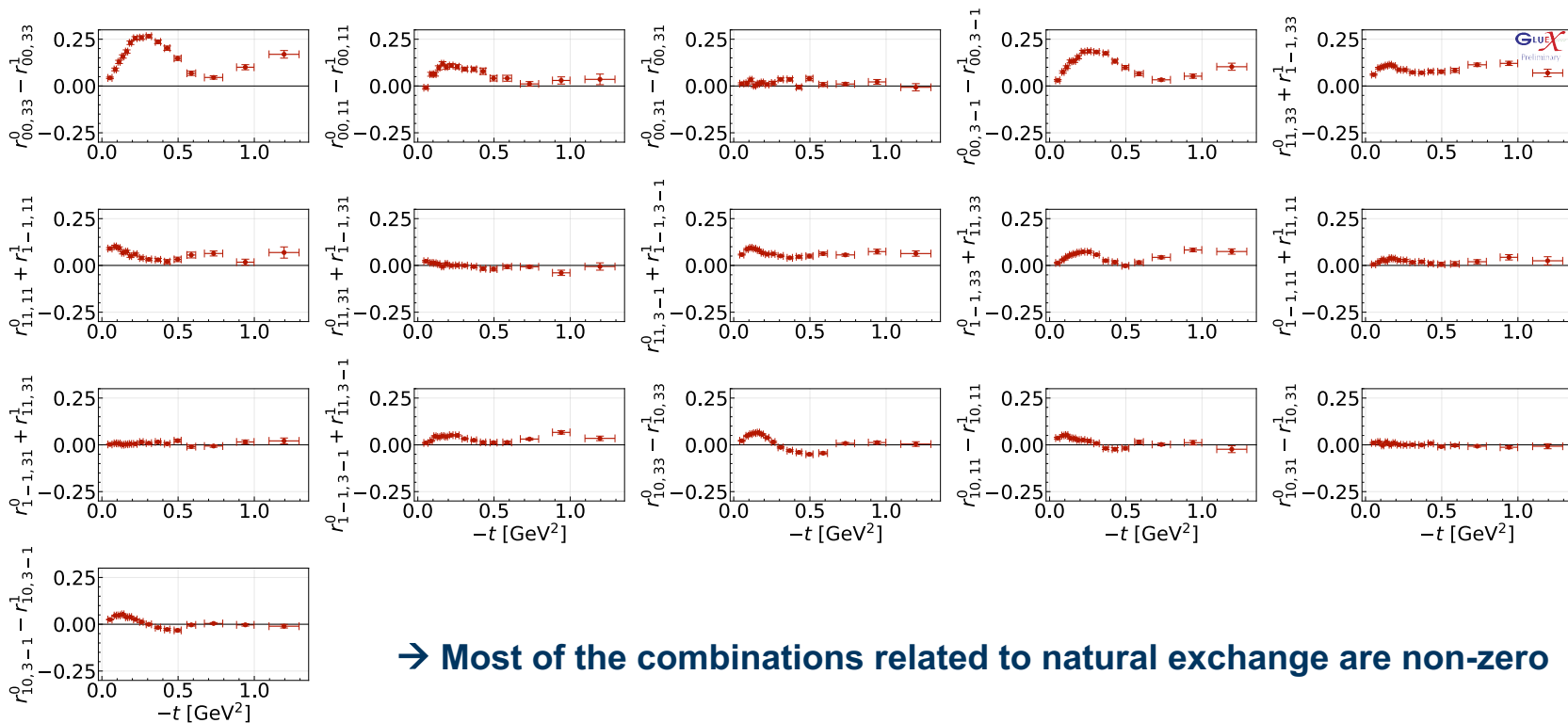
$$r_{00,33}^0 + r_{00,33}^1 = 2(|U_{0,3}|^2 + |U_{0,-3}|^2) \quad (\text{purely unnatural exchange})$$

$$\tilde{r}_{10,31}^0 + \tilde{r}_{10,31}^1 = \frac{1}{2} [(N_{1,-3} + N_{-1,-3}^*) U_{0,-1}^* - (N_{1,-1} + N_{-1,-1}) U_{0,-3}^*] \quad (\text{interference})$$

V. Shastry, V. Mathieu

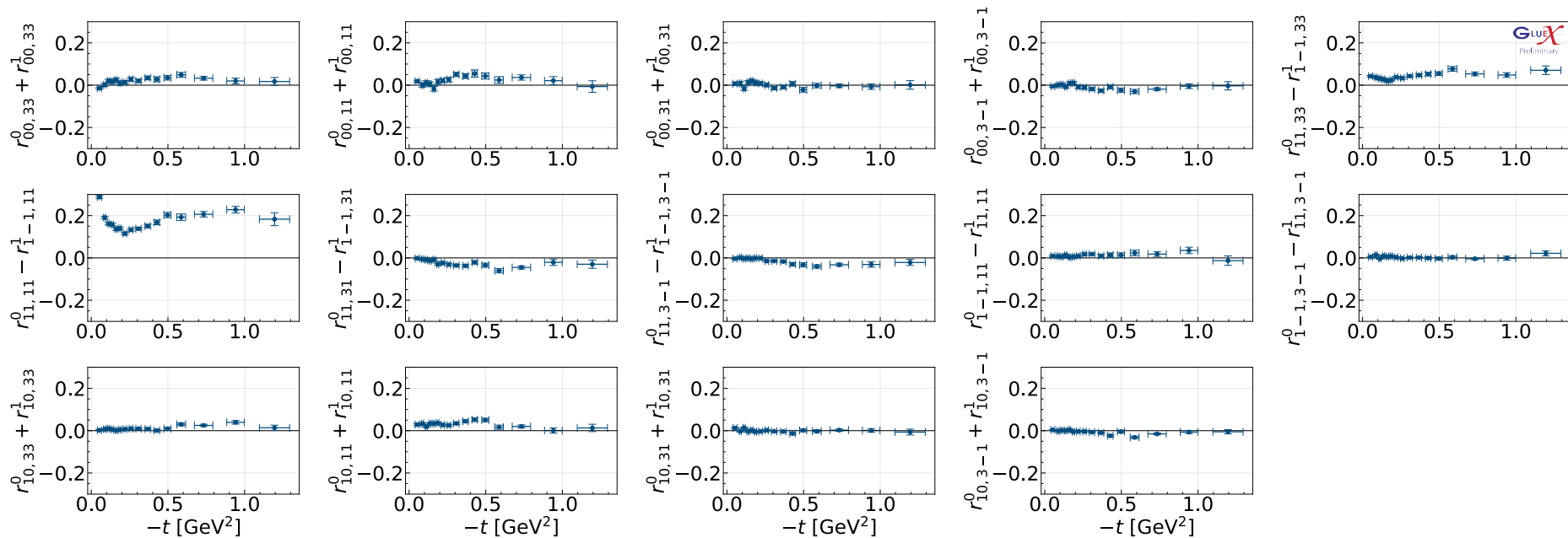


# Natural exchange



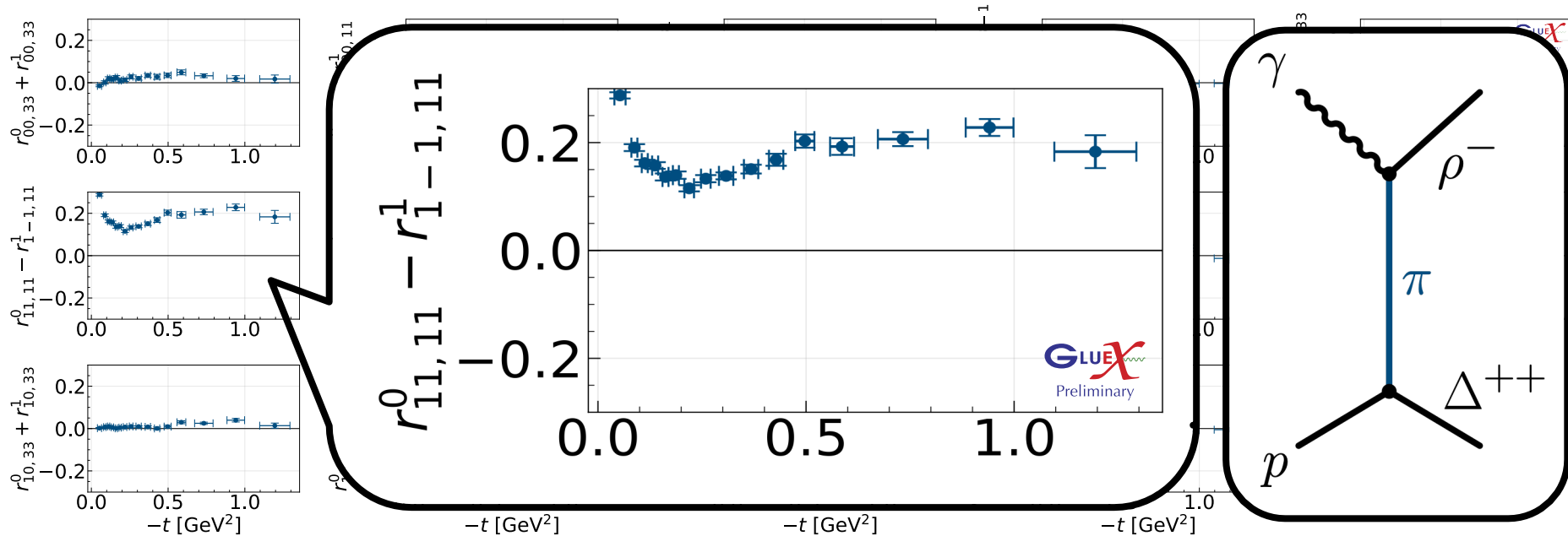
→ Most of the combinations related to natural exchange are non-zero

# Unnatural exchange



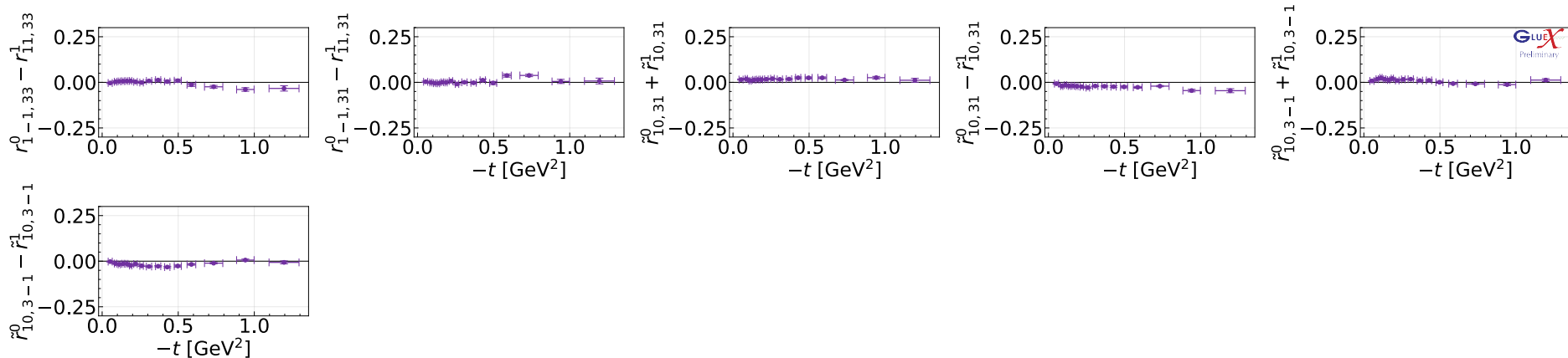
→ Small unnatural exchange contributions

# Unnatural exchange



→ Small unnatural exchange contributions

# Interference



→ No strong interference between natural and unnatural exchange

→ This also confirms that only one exchange dominates

→ In this case, we can try to fit a simplified factorized model

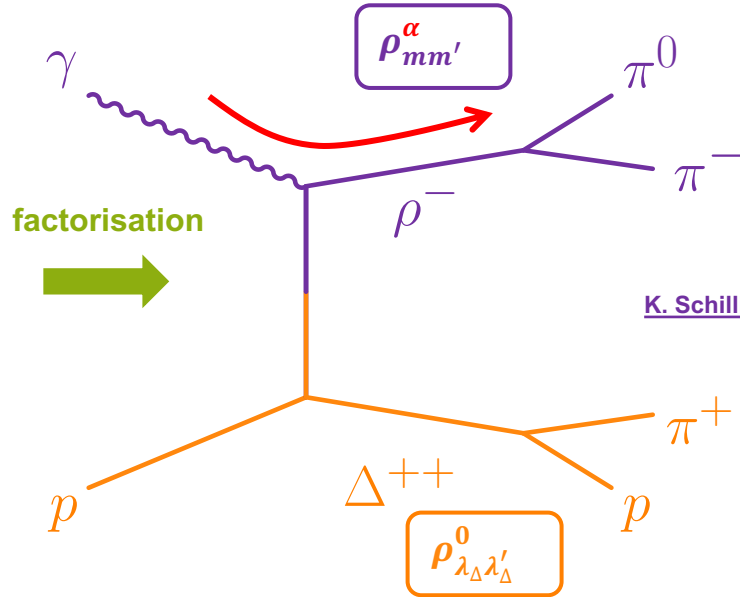
# Factorized Model

# Factorized fit model

In case of factorization photon talks only to meson!

**55 fit parameters**

$r_{00,33}^0, r_{11,33}^0, r_{11,11}^0, r_{1-1,33}^0, r_{1-1,33}^1, r_{1-1,11}^1, \dots$   
 $r_{00,33}^1, r_{00,11}^0, r_{11,33}^1, r_{11,11}^1, r_{1-1,33}^1, r_{1-1,11}^1, r_{10,33}^1, r_{10,11}^1, \dots$   
 $r_{1-1,33}^2, r_{1-1,11}^2, r_{1-1,31}^2, r_{1-1,3-1}^2, r_{10,33}^2, r_{00,31}^2, r_{00,3-1}^2, r_{11,31}^2, \dots$



factorisation  
→

**9 fit parameters**

$\rho_{00}^0, \rho_{10}^0, \rho_{1-1}^0$   
 $\rho_{11}^1, \rho_{00}^1, \rho_{10}^1, \rho_{1-1}^1$   
 $\rho_{10}^2, \rho_{1-1}^2$

K. Schilling, P. Seyboth & G. Wolf (1970), Nuclear Physics B, 15(2), 397–412.

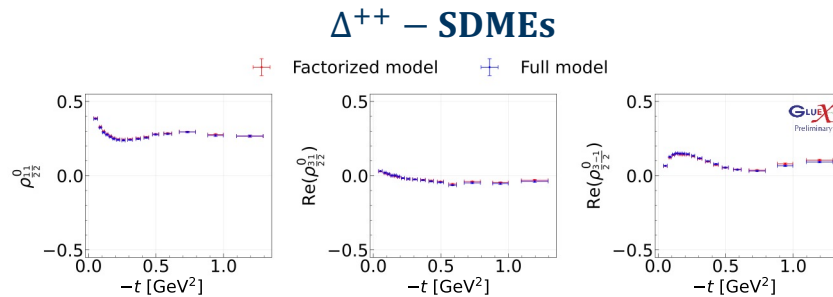
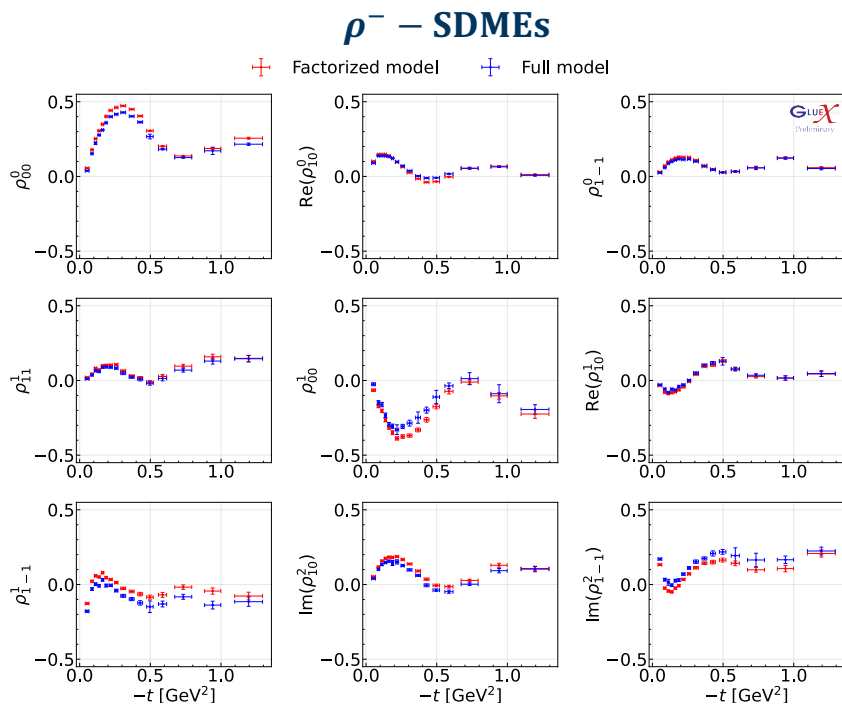
**3 fit parameters**

$\frac{\rho_{11}^0}{2\ 2}, \frac{\rho_{31}^0}{2\ 2}, \frac{\rho_{3-1}^0}{2\ 2}$

F. Afzal et al. (2025), Phys. Lett. B, 863, 139368.

$$I_{tot} = (I_{0,\rho} + \sum_{\alpha=1,2} P_\alpha I_{\alpha,\rho}) I_{0,\Delta}$$

# Comparison between factorized and full model

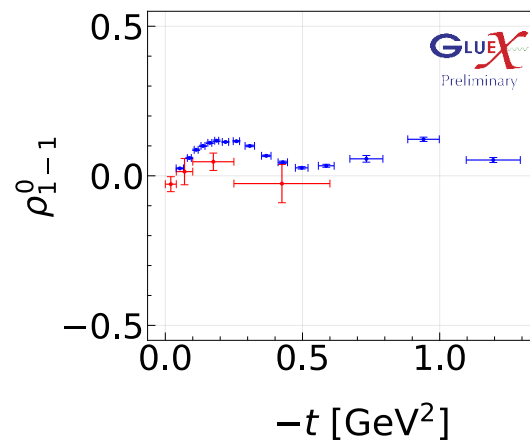
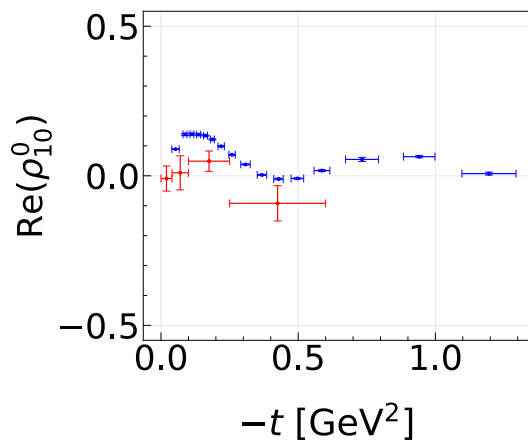
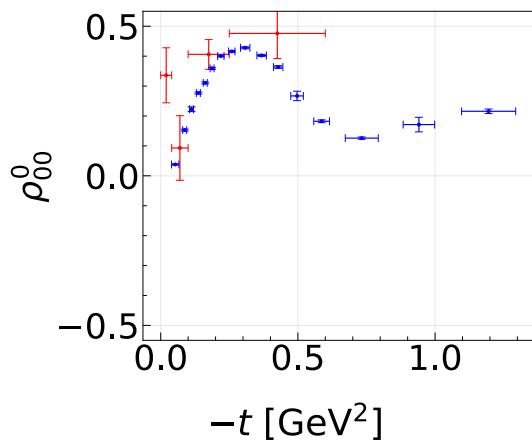


→ Overall good agreement between full model and factorized model

# Results for $\rho^-$ compared to SLAC

J. Abramson et al. (1976) Phys. Rev. Lett., 36(24),1432-1434.

SLAC GLUEX Preliminary



→ Within the errors, our results agree with the previous measurement for unpolarized SDMEs (visible systematic trend)



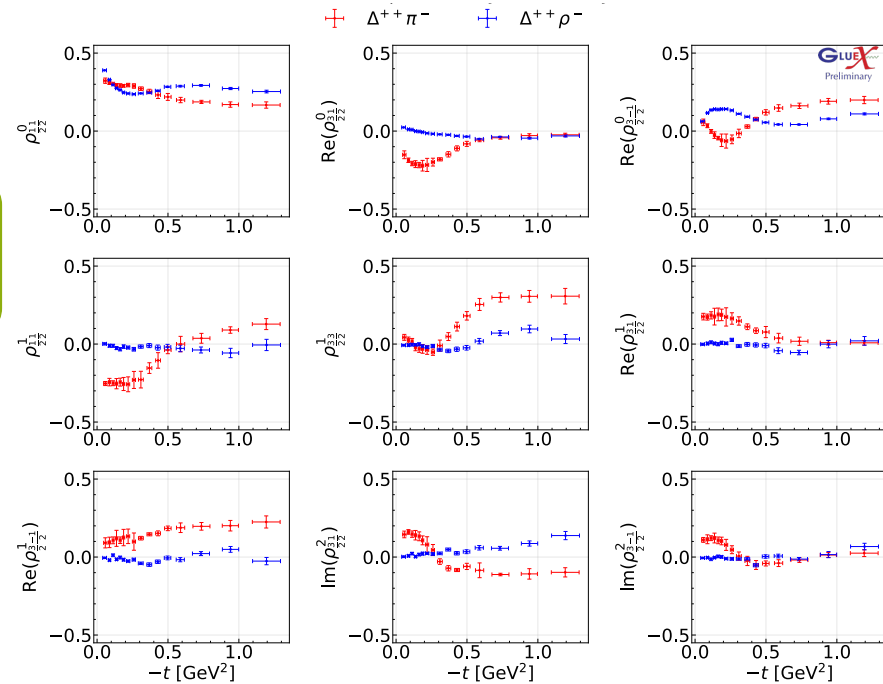
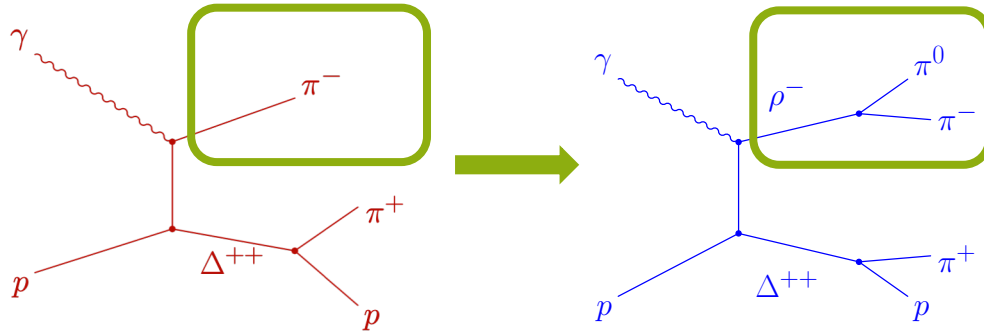
# Conclusion

- **Photoproduction is an alternative mechanism to search for hybrid mesons**
- **Polarized SDMEs are an important tool to understand the production mechanism**
- **First results of the SDMEs of the reaction  $\gamma + p \rightarrow \rho^- \Delta^{++}$  in GlueX-I data**
- **Within uncertainties, the results are consistent with previous measurements for unpolarized SDMEs from SLAC**
- **Full model (55 fit parameters) and factorized model (12 fit parameters) in good agreement**
- **Factorized model Ansatz is reasonable**
- **Results could also be used for other studies ( $\Delta^{++} \eta \pi$ ,  $\Delta^{++} \eta' \pi$ ,  $\Delta^{++} \pi \pi \pi$ )**

# Appendix

# Comparison between $\Delta^{++}\pi^{-}$ and $\Delta^{++}\rho^{-}$

F. Afzal et al. (GLUOX)  
(2025), *Phys. Lett. B*, 863, 139368.



→ Different production mechanisms result in different SDME dependences on  $-t$

# Reduced Spin Density Matrix

- Given a joint system  $\Delta^{++}\rho^-$  the reduced density matrix for subsystem  $\Delta^{++}$  is:

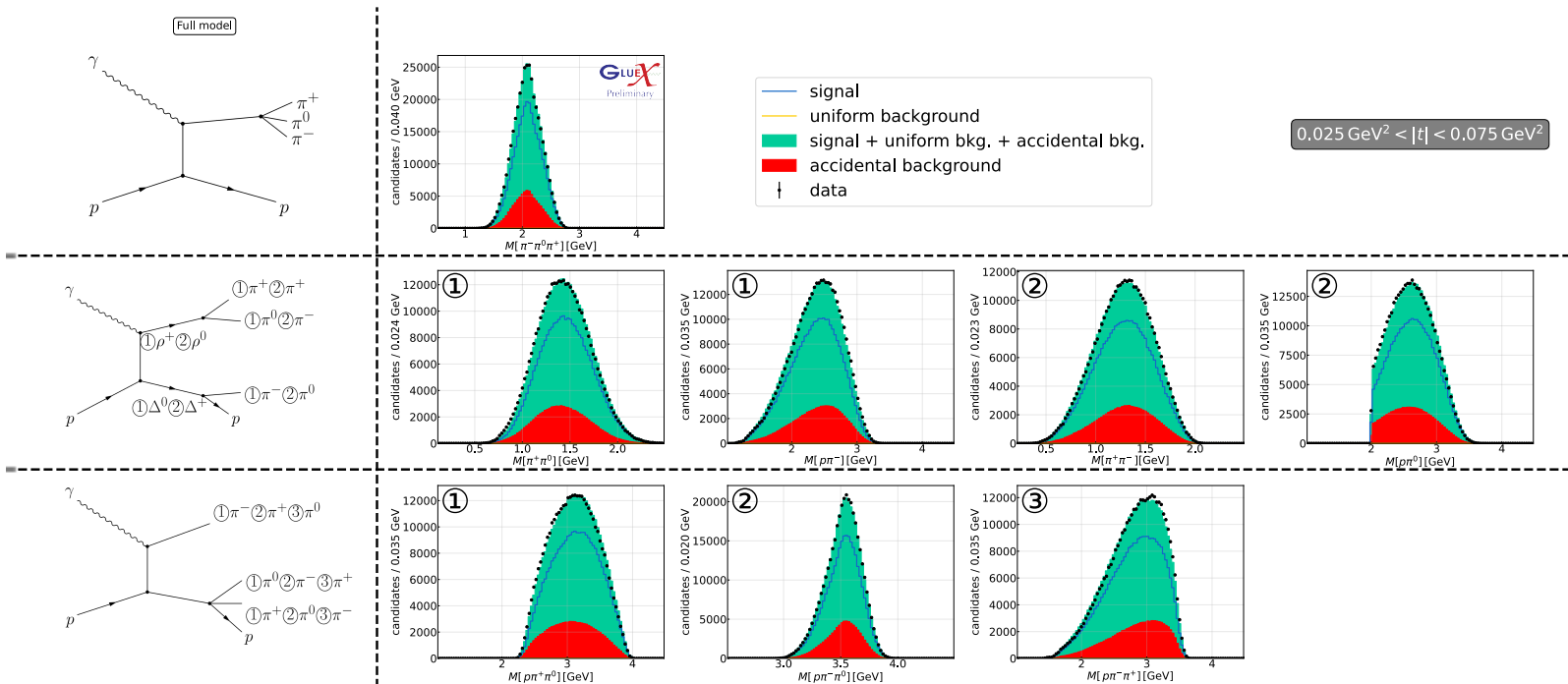
$$\rho_{\Delta^{++}} = \text{Tr}_{\rho^-}(\rho_{\Delta^{++}\rho^-}) = \sum_m \rho_{mm, \lambda_{\Delta} \lambda'_{\Delta}}$$

- $\rho_{\Delta^{++}}$  allows calculation of expectation values for observables acting only on subsystem  $\Delta^{++}$ , yielding the same results as using the total density matrix

- Example:  $\rho_{00}^{0, \rho^-} = \sum_{\lambda} \rho_{00, \lambda \lambda}^0 = (\rho_{00, -3 -3}^0 + \rho_{00, -1 -1}^0 + \rho_{00, 11}^0 + \rho_{00, 33}^0) = (2r_{00, 11}^0 + 2r_{00, 33}^0)$
- One can also show with the parity relation that:  $\text{Tr}(\rho_{\rho^-}^0) = \text{Tr}(\rho_{\Delta^{++}}^0)$ ,  $\text{Tr}(\rho_{\rho^-}^1) = \text{Tr}(\rho_{\Delta^{++}}^1)$

$$\Rightarrow \rho_{00}^1 = 2\left(\rho_{\frac{1}{2}\frac{1}{2}}^1 + \rho_{\frac{3}{2}\frac{3}{2}}^1 - \rho_{11}^1\right)$$

# Fit evaluation



→ Overall good agreement between data and fit

# Event selection

## Vertex and Quality:

Cut on vertex position

$$QF_{shower} > 0.5$$

$$N_{unused\ tracks} \leq 1$$

$$N_{unused\ shower} \leq 3$$

## Kinematics:

$$\chi^2/NDF < 5$$

$$8.2\text{ GeV} < E_{beam} < 8.8\text{ GeV}$$

$$-0.01\text{ GeV}^2 < M_{miss}^2 < 0.01\text{ GeV}^2$$

$$p_{\pi^+,z} < 0.2\text{ GeV}$$

$$0.025\text{ GeV}^2 < -t < 1.4\text{ GeV}^2$$

## Mass windows:

$$0.62\text{ GeV} < M(\pi^-\pi^0) < 0.93\text{ GeV}$$

$$1.10\text{ GeV} < M(\pi^+p) < 1.35\text{ GeV}$$

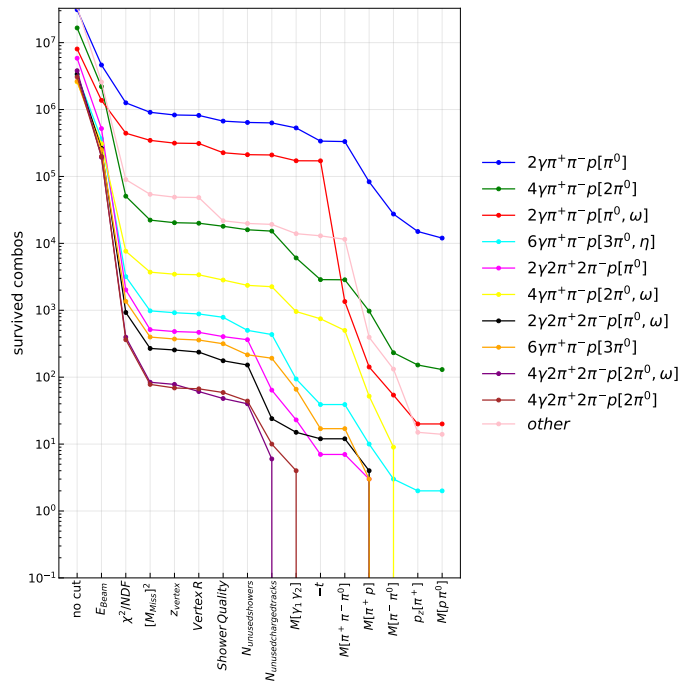
$$0.12\text{ GeV} < M(\gamma\gamma) < 0.15\text{ GeV}$$

$$0.9\text{ GeV} < M(\pi^-\pi^0\pi^+)$$

$$2.0\text{ GeV} < M(\pi^0p)$$

# Effectiveness of event selection

$N_t / \sum_t N_t$ [%]	Topology
98.644	$2\gamma\pi^+\pi^-p[\pi^0]$
0.847	$4\gamma\pi^+\pi^-p[2\pi^0]$
0.149	$2\gamma\pi^+\pi^-p[\pi^0, \omega]$
0.009	$6\gamma\pi^+\pi^-p[3\pi^0, \eta]$
0.000	$2\gamma 2\pi^+2\pi^-p[\pi^0]$
0.027	$4\gamma\pi^+\pi^-p[2\pi^0, \omega]$
0.000	$2\gamma 2\pi^+2\pi^-p[\pi^0, \omega]$
0.000	$6\gamma\pi^+\pi^-p[3\pi^0]$
0.000	$4\gamma 2\pi^+2\pi^-p[2\pi^0, \omega]$
0.000	$4\gamma 2\pi^+2\pi^-p[2\pi^0]$
0.324	other

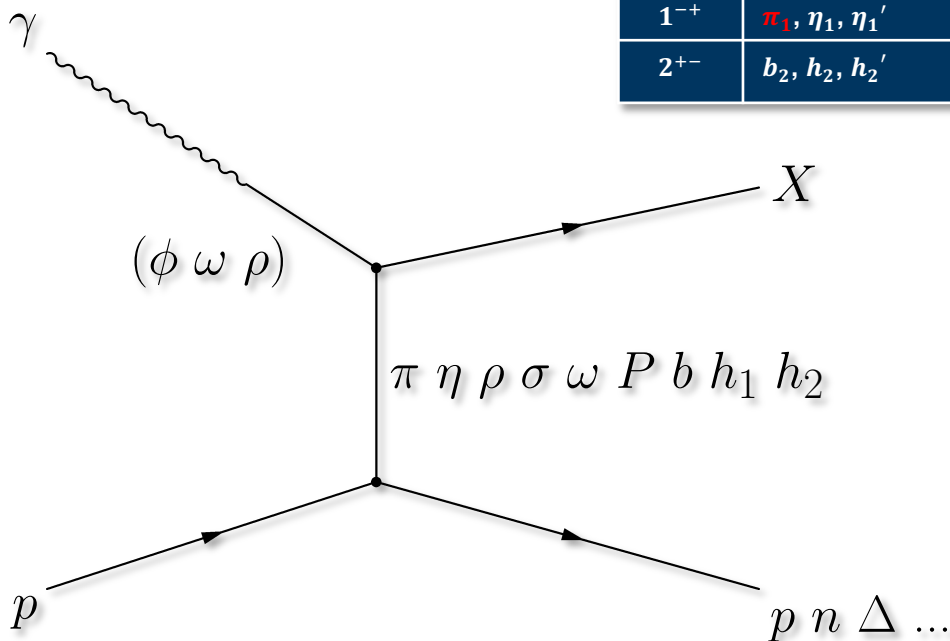


→The event selection is effective: background processes not corresponding to  $\pi^+\pi^-\pi^0p$  final states are significantly suppressed by the applied cuts (background < 1.4 %)

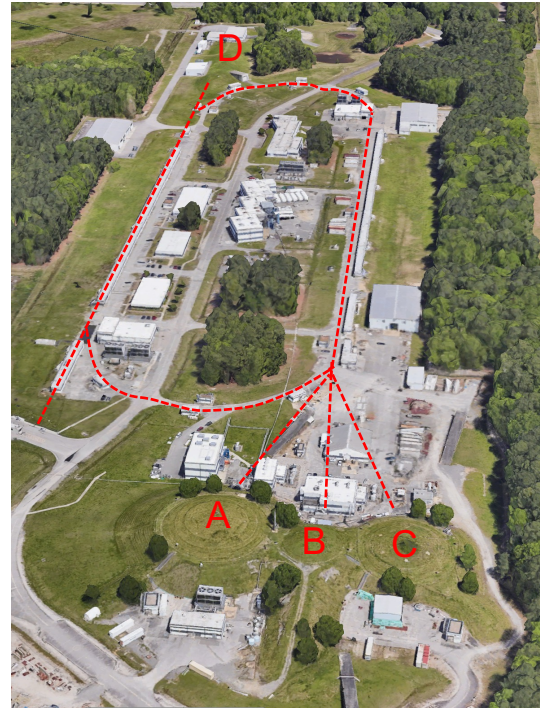
# Photoproduction

- Photoproduction is a complementary production process to search for hybrid mesons compared to ongoing searches at other facilities
- Different reggeons with different quantum numbers are exchanged in t-channel process
  - Can produce mesons of any  $J^{PC}$
- Photon Polarization → constrain on production processes, studying of hadron properties

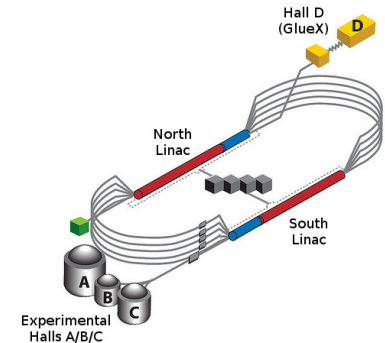
$J^{PC}$	Exotic Meson
$0^{+-}$	$b_0, h_0, h_0'$
$1^{-+}$	$\pi_1, \eta_1, \eta_1'$
$2^{+-}$	$b_2, h_2, h_2'$



# CEBAF at Jefferson Lab

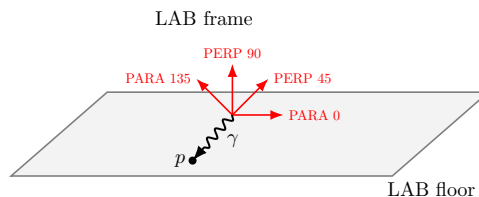
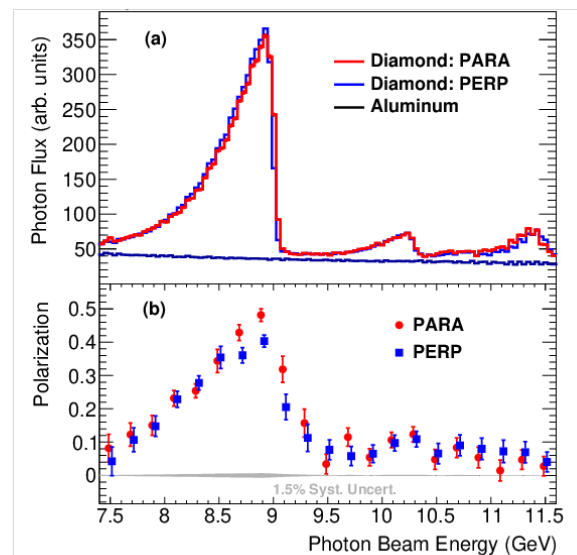
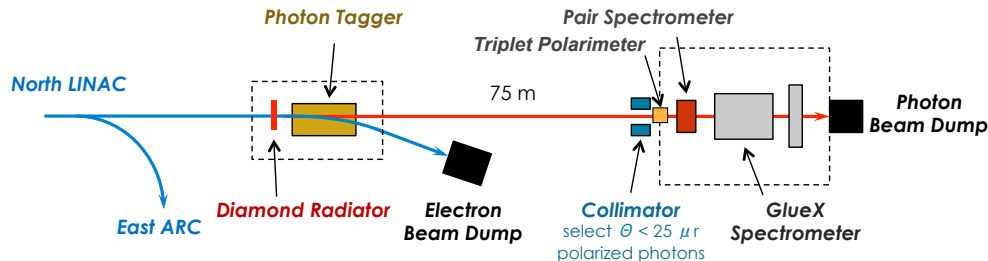


- $E_e < 12$  GeV  
electron beam
- $I_e$  up to  $2\mu\text{A}$
- GlueX in Hall D
- CLAS in Hall B

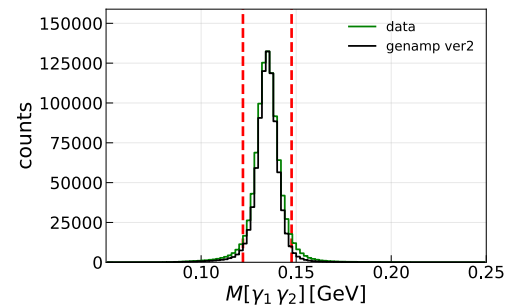
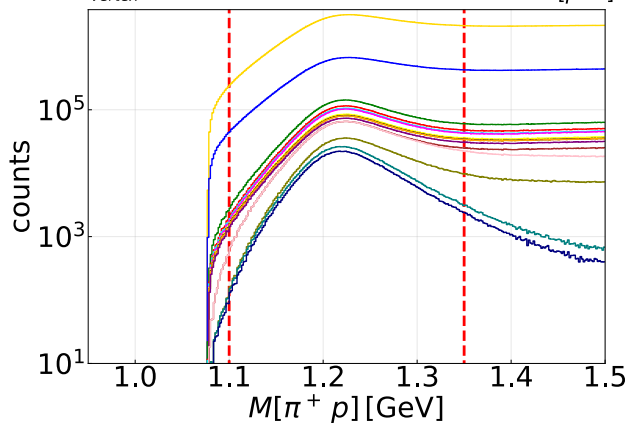
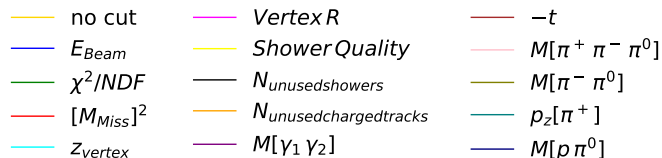
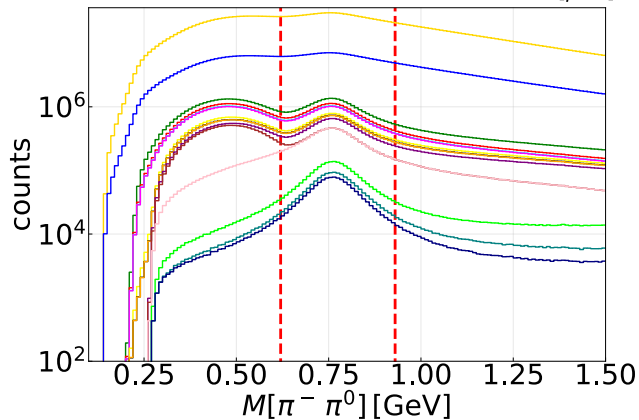
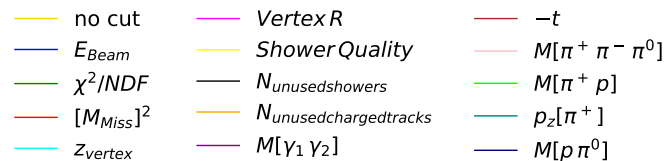


# Photon Beam Line

- Coherent Bremsstrahlung on thin diamond radiator
- Collimator to suppress incoherent part
- Linear polarization in peak ( $P \sim 35\%$ ) measured by Triplet polarimeter
- Beam energy is tagged, photon flux measured close to spectrometer
- Polarization rotated into 4 different orientations (parallel and perpendicular)
- $I_\gamma \sim 1 - 5 \cdot 10^7 \frac{\gamma}{s}$  (in peak)



# Invariant mass cuts

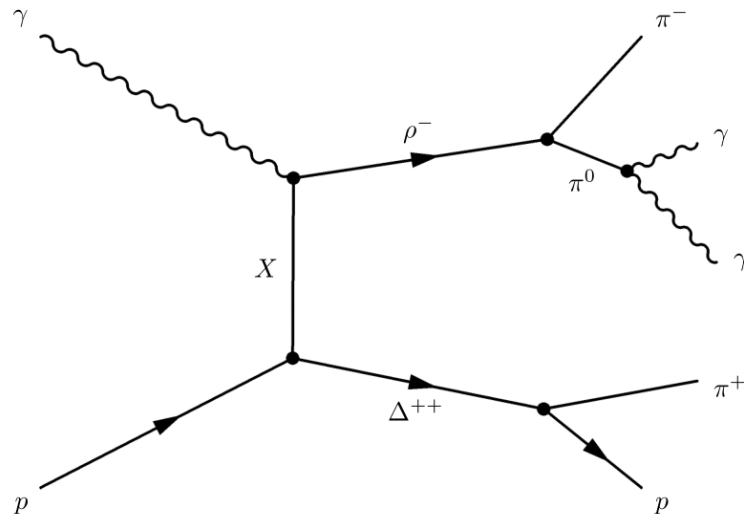


# Process of interest

- Study of exclusive photoproduction of  $\Delta^{++}\rho^{-}$
- Data from GlueX-I (2017+2018)

## Dataset contains:

- Applied kinematic fit (momentum, vertex)
- No mass constraint on  $\pi^0$
- Event topology:  $p$ ,  $\pi^+$ ,  $\pi^-$  and 2 neutral showers
- up to 3 additional charged tracks allowed
- $\pm 4$  beam bunches at each side



# Intensities

$$W(\Omega_\pi, \Omega_p, \Phi) = \frac{3}{4\pi} (W^0(\Omega_\pi, \Omega_p) - P_Y \cos(2\Phi) W^1(\Omega_\pi, \Omega_p, \Phi) - P_Y \sin(2\Phi) W^2(\Omega_\pi, \Omega_p, \Phi))$$

## Full model – Double SDME

$$W^0(\Omega_\pi, \Omega_p) = \cos^2(\vartheta_\pi) [W_{00}^0(\Omega_p) - \bar{W}_{00}^0(\Omega_p)] + \sin^2(\vartheta_\pi) [W_{11}^0(\Omega_p) - \bar{W}_{11}^0(\Omega_p)] \\ - \sin^2(\vartheta_\pi) (\cos(2\phi_\pi) [W_{1-1}^0(\Omega_p) - \bar{W}_{1-1}^0(\Omega_p)] + \sin(2\phi_\pi) \bar{W}_{1-1}^0(\Omega_p)) \\ - \sqrt{2} \sin(2\vartheta_\pi) (\cos(\phi_\pi) [W_{10}^0(\Omega_p) - \bar{W}_{10}^0(\Omega_p)] + \sin(\phi_\pi) \bar{W}_{10}^0(\Omega_p))$$

$W^1(\Omega_\pi, \Omega_p)$  has same form as  $W^0(\Omega_\pi, \Omega_p)$  due to the same parity relations

$$W^2(\Omega_\pi, \Omega_p) = \cos^2(\vartheta_\pi) \bar{W}_{00}^2(\Omega_p) + \sin^2(\vartheta_\pi) \bar{W}_{11}^2(\Omega_p) \\ + \sin^2(\vartheta_\pi) (\sin(2\phi_\pi) [W_{1-1}^2(\Omega_p) - \bar{W}_{1-1}^2(\Omega_p)] - \cos(2\phi_\pi) \bar{W}_{1-1}^2(\Omega_p)) \\ + \sqrt{2} \sin(2\vartheta_\pi) (\sin(\phi_\pi) [W_{10}^2(\Omega_p) - \bar{W}_{10}^2(\Omega_p)] + \cos(\phi_\pi) \bar{W}_{10}^2(\Omega_p))$$

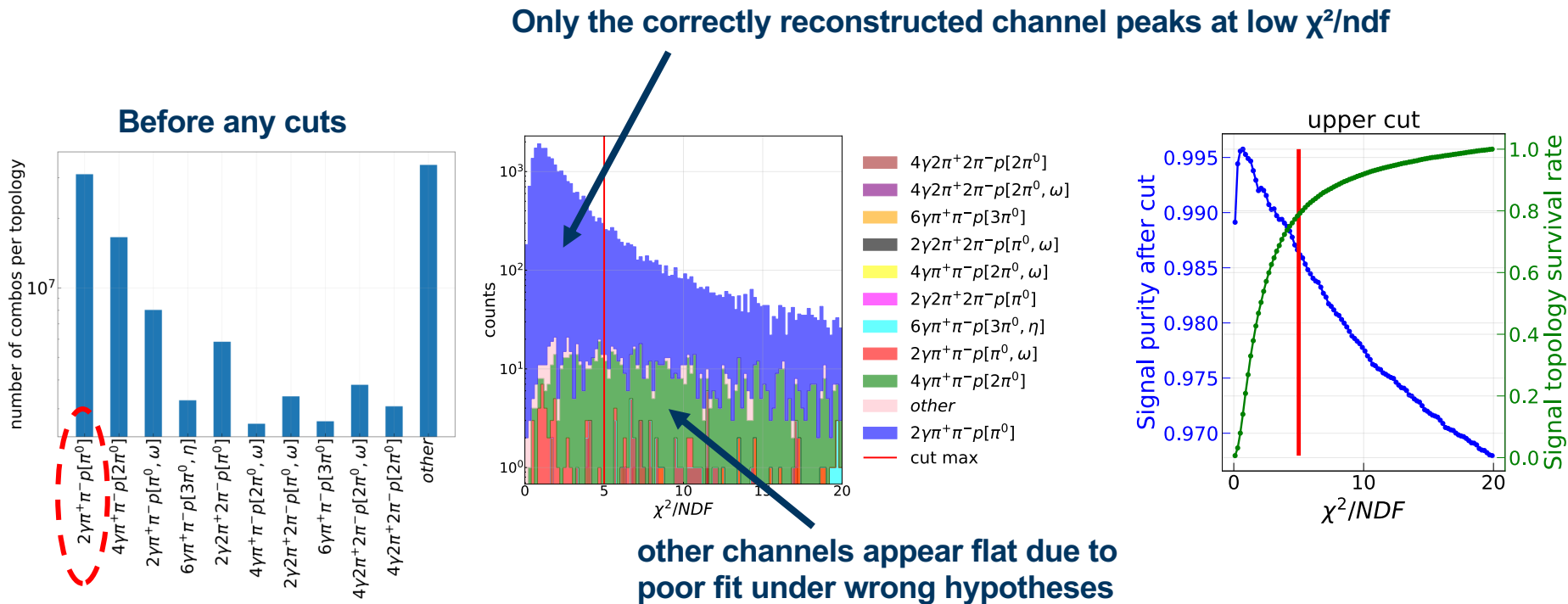
$$W_{mm'}^\alpha(\Omega_p) = r_{mm'3}^\alpha \sin^2(\vartheta_p) + r_{mm'1}^\alpha \left( \frac{1}{3} + \cos^2(\vartheta_p) \right)$$

$$\bar{W}_{mm}^\alpha(\Omega_p) = \frac{2}{\sqrt{3}} \left[ r_{mm'3}^\alpha \cos(\varphi_p) \sin(2\vartheta_p) + r_{mm'3-1}^\alpha \cos(2\varphi_p) \sin^2(\vartheta_p) \right]$$

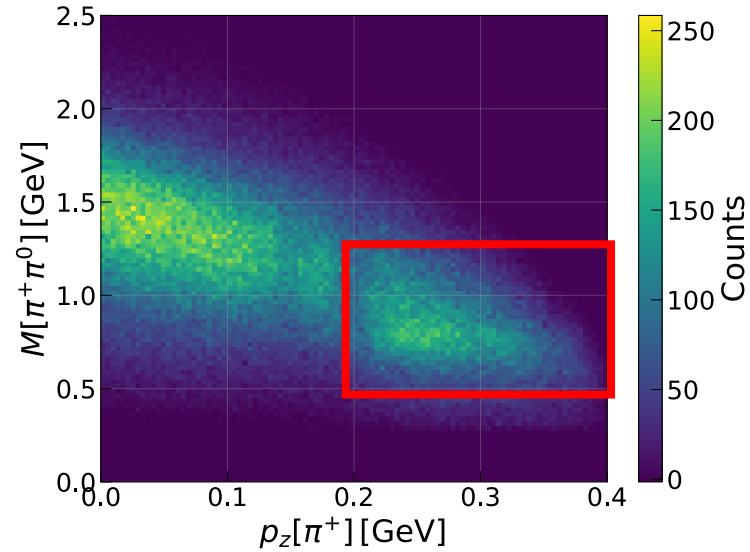
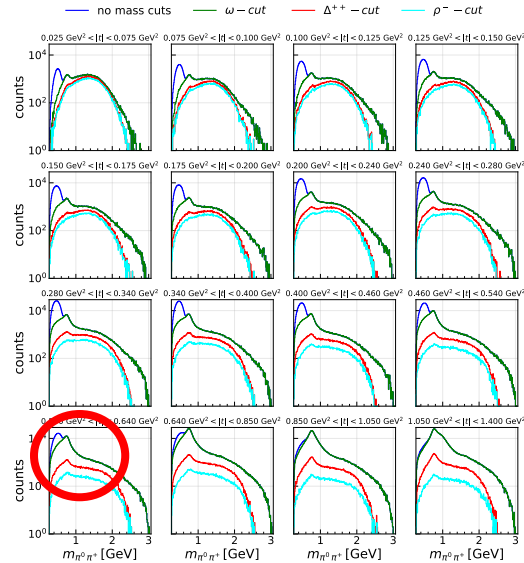
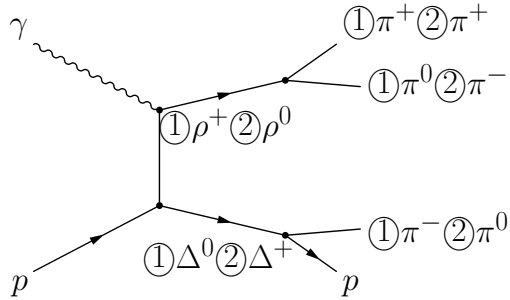
$$\bar{W}_{mm}^\alpha(\Omega_p) = \frac{2}{\sqrt{3}} \left[ \bar{r}_{mm'31}^\alpha \sin(\varphi_p) \sin(2\vartheta_p) + \bar{r}_{mm'3-1}^\alpha \sin(2\varphi_p) \sin^2(\vartheta_p) \right]$$

→  $r_{mm'\lambda_\Delta\lambda'_\Delta}^\alpha$  is a linear combination of one to four  $\rho_{mm'\lambda_\Delta\lambda'_\Delta}^\alpha$

# Bggen study

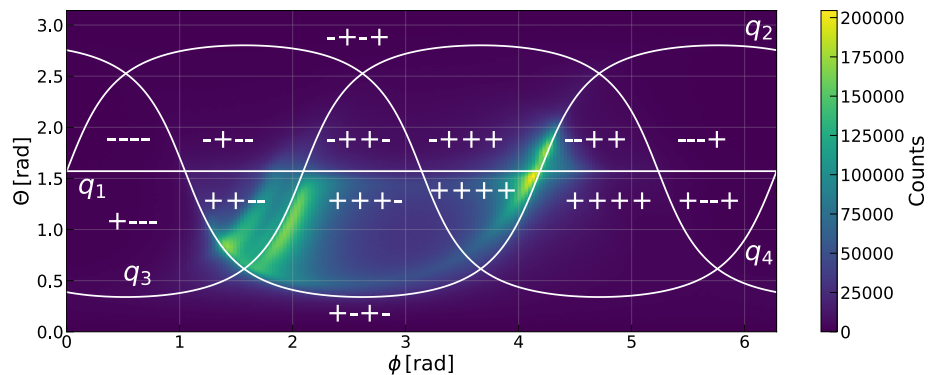


# $\rho^0/\rho^+$ background



→ Cut on  $p_{\pi^+,z} < 0.2$  GeV

# Great-circle Plot



$$r = \sqrt{x^2 + y^2 + z^2}$$

$$\theta = \tan^{-1} \frac{\sqrt{x^2 + y^2}}{z}$$

$$\phi = \tan^{-1} \frac{y}{x}$$

Event selection

